CHINESE OPTICS LETTERS

Vol. 19, No. 7 | July 2021

# Robust modal phase matching in subwavelength $x$-cut and $z$-cut lithium niobate thin-film waveguides

Lingzhi Peng (彭凌志)[1], Lihong Hong (洪丽红)[1], Baoqin Chen (陈宝琴)[1], Peng He (何 鹏)[2,3**], and Zhiyuan Li (李志远)[1*]

[1] School of Physics and Optoelectronics, South China University of Technology, Guangzhou 510641, China

[2] Guangdong Full-Spectra Laser Technology Co., Ltd., Dongguan 523808, China

[3] Dongguan Sanhang Innovation Research Institute, Dongguan 523808, China

*Corresponding author: phzyli@scut.edu.cn

**Corresponding author: hfirst@163.com

Received November 4, 2020 | Accepted December 19, 2020 | Posted Online March 30, 2021

We use the nonlinear coupled-mode theory to theoretically investigate second-harmonic generation (SHG) in subwavelength $x$-cut and $z$-cut lithium niobate (LN) thin-film waveguides and derive the analytical formula to calculate SHG efficiency in $x$-cut and $z$-cut LN thin-film waveguides explicitly. Under the scheme of optimal modal phase matching (MPM), two types of LN thin films can achieve highly efficient frequency doubling of a 1064 nm laser with a comparable conversion efficiency due to very consistent modal field distribution of the fundamental wave and second-harmonic wave with efficient overlap between them. Such a robust MPM for high-efficiency SHG in both the subwavelength $x$-cut and $z$-cut LN thin-film waveguides is further confirmed in a broad wavelength range, which might facilitate design and application of micro–nano nonlinear optical devices based on the subwavelength LN thin film.

**Keywords:** lithium niobate thin film; modal phase matching; nonlinear coupled-mode theory; second-harmonic generation.
**DOI:** 10.3788/COL202119.071902

## 1. Introduction

A series of integrated nonlinear photonic platforms that enables tight confinement of light at the micro/nanoscale has been constructed to achieve efficient nonlinear frequency conversion. Among them, lithium niobate (LN) has garnered significant attention for its excellent electro-optical, quadradic optical nonlinearity properties and wide transparency range. A variety of nanophotonic devices and systems based on LN thin films have been fabricated and realized, including waveguides[1–5], electro-optic modulators[6,7], microdisk resonators[8–11], and photonic crystal cavities[12–14]. In particular, subwavelength LN thin-film waveguides with high-index contrast have raised extensive and intensive interest in facilitating second-harmonic generation (SHG) because they own a much smaller confinement size of light energy than bulk LN and a more efficient spatial overlap between interacting fundamental wave (FW) and second-harmonic wave (SHW), which contribute to strong nonlinear interactions when light transports in the waveguide.

In general, to obtain significant efficiency of SHG in crystal, the interacting waves in crystal need to meet the phase-matching (PM) condition by using the birefringence PM scheme or quasi-PM scheme[15,16]. In thin-film slab structures, the PM conditions of interacting optical modes are determined not only by the dispersion of LN material but also by the geometric configuration parameters and the degree of light confinement[17], leading to the scheme of modal PM (MPM). Besides, to achieve a high conversion efficiency of SHG in LN thin-film waveguides, one should manage to make full use of the large non-zero effective nonlinear coefficients of LN and excellent spatial overlap between the FW mode and SHW mode[17–20].

MPM in LN thin films has been studied before, but lacks theoretical analysis of several critical features of SHG such as conversion efficiency[5]. In our previous work, we developed a systematic theory for analyzing and evaluating the quadratic nonlinear process in $z$-cut LN thin-film waveguides[17]. However, for LN thin-film waveguides cut in other directions, considering the complex anisotropy of nonlinear polarizability tensor in the crystal and the strong confinement of the optical field in the thin-film structure, the distribution of modal field and the mutual coupling between them would be very complicated and diversified. To exploit more feasible and effective routes for highly efficient frequency conversion, much work still exists that needs to be supplemented. In this Letter, we use the well-established MPM theory, fully considering both the natural anisotropy in linear permittivity, refractive index, and second-order nonlinear susceptibility tensor, and derive a set of analytical mathematical formulas of SHG conversion efficiency

in $x$-cut LN thin-film waveguides. We find that both the $x$-cut and $z$-cut LN thin-film waveguides can achieve comparable highly efficient frequency doubling in a wide spectral range (including the most useful wavelengths 1064 and 1550 nm), and therefore fruitful configuration of LN waveguides can be harnessed for practical applications.

## 2. Theoretical Model

Figure 1 illustrates a particular configuration of the LN thin-film waveguide used for SHG. The waveguide is a three-slab structure composed of a substrate layer with refractive index $n_0$, a cladding layer with refractive index $n_2$, and an LN thin film with thickness $h$. In particular, the coordinate axes are set to be collinear with the principal crystalline orientations. For $x$-cut LN ($z$-cut LN), the $x$ axis ($z$-axis) is collinear with the optical axis (extraordinary crystalline axis) of LN. Both the FW pump light and SHW signal light travel along the $y$ axis.

Two independent electromagnetic modes exist in the waveguide, which are denoted as TE modes (containing $E_x$, $H_y$, $H_z$ components) and TM modes (containing $H_x$, $E_y$, $E_z$ components), respectively. In our specific system of $x$-cut LN thin-film waveguides, the TE mode can be called the extraordinary light (EL) mode with refractive index $n_e$, where the value of $n_e$ follows the Sellmieier equation[21]. By combining Maxwell's equations with the boundary conditions for electromagnetic fields at two interfaces of LN waveguides, the dispersion equation for TE modes can be derived as

$$k_0 h(n_e^2 - n_{\text{eff}}^2)^{1/2} = m\pi + \arctan\left(\frac{n_{\text{eff}}^2 - n_0^2}{n_e^2 - n_{\text{eff}}^2}\right)^{1/2} + \arctan\left(\frac{n_{\text{eff}}^2 - n_2^2}{n_e^2 - n_{\text{eff}}^2}\right)^{1/2}. \quad (1)$$

Here, the integer $m$ ($m = 0, 1, 2 \ldots$) represents the mode number. $k_0 = \omega/c$, where $c$ and $k_0$ are the speed of light and wave vector of light in vacuum, respectively. $n_{\text{eff}}$ denotes the effective refractive index for guided modes; for the TE mode, $n_{\text{eff}} = n_e \sin\theta$ ($\theta$ being the incident angle). $\Delta k = 2\beta_1 - \beta_2$ ($\beta_1 = k_0 n_{\text{eff}}^{\omega}$, $\beta_2 = 2k_0 n_{\text{eff}}^{2\omega}$) denotes the phase mismatching between the FW mode and SHW modes. The symbol $L$ denotes the transport distance, and $E_{1x}$, $E_{2x}$ are the normalized electric field distributions of the FW and SHW modes along the $x$-axis direction, respectively. When $\Delta k = 0$, under small signal conditions, the conversion efficiency of SHG for the EL + EL → EL PM scheme can be expressed as

$$\eta = \frac{P_{2\omega}}{P_{1\omega}} = \frac{\omega_1^2 L^2}{n_{\text{eff}}^{\omega} n_{\text{eff}}^{2\omega} c^2} |\kappa_2|^2 |A_1(0)|^2 \frac{\int |E_{2x}(z)|^2 \mathrm{d}z}{\int |E_{1x}(z)|^2 \mathrm{d}z}. \quad (2)$$

For generally large signal situations, we have

$$\eta = \frac{P_{2\omega}}{P_{1\omega}} = \frac{n_{\text{eff}}^{2\omega}|\kappa_2|}{n_{\text{eff}}^{\omega}|\kappa_1|} \tanh^2\left(\frac{2\pi}{n_{\text{eff}}^{2\omega}\lambda_{\omega}} \sqrt{|\kappa_1||\kappa_2|}|A_1(0)|L\right) \times \frac{\int |E_{2x}(z)|^2 \mathrm{d}z}{\int |E_{1x}(z)|^2 \mathrm{d}z}. \quad (3)$$

Here, $A_1(0)$ is the electric-field amplitude of the input FW pump light. $\kappa_1$ and $\kappa_2$ are quadratic nonlinear coupling coefficients in the units of pm/V, which are closely related to the convolution of the TE field distributions of FW and SHW in LN thin-film waveguides and the nonlinear susceptibility tensor $\chi^{(2)}$[17]. In the $x$-cut LN thin-film system, the form of $d$ ($d = \chi^{(2)}/2$) can be rewritten as

$$\begin{pmatrix} d_{33} & d_{31} & d_{31} & 0 & 0 & 0 \\ 0 & 0 & 0 & -d_{22} & 0 & d_{31} \\ 0 & -d_{22} & d_{22} & 0 & d_{31} & 0 \end{pmatrix}, \quad (4)$$

where $d_{33} = 27$ pm/V, $d_{31} = 5.45$ pm/V, and $d_{22} = 2.76$ pm/V.

For the EL + EL → EL PM scheme, both the FW pump light and SHW signal light are EL (containing field components $E_{1x}, E_{2x}$). Therefore, the nonlinear coupling coefficients $\kappa_1$ and $\kappa_2$ have the form

$$\kappa_1 = 2\int d_{33}(E_{1x}^{\star})^2 E_{2x}\mathrm{d}z \Big/ \int E_{1x}^{\star} E_{1x}\mathrm{d}z, \quad (5)$$

$$\kappa_2 = 2\int d_{33}(E_{1x})^2 E_{2x}^{\star}\mathrm{d}z \Big/ \int E_{2x}^{\star} E_{2x}\mathrm{d}z. \quad (6)$$

Now, we have derived the accurate analytical formula for calculating the efficiency of SHG in $x$-cut LN thin-film waveguides. Equations (2) and (3) clearly reveal that the conversion efficiency is positively correlated with the nonlinear coupling coefficients $\kappa_1$, $\kappa_2$, and these two quantities play a similar role in the LN thin-film waveguide as the effective nonlinear coefficient plays in bulk crystal[22,23].

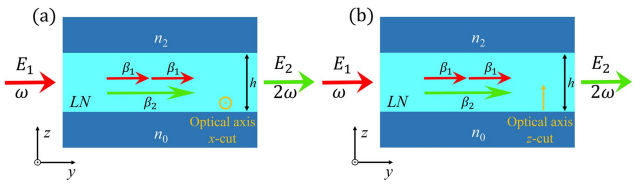


**Fig. 1.** Structures of the LN thin-film waveguide and the schemes of the phase matching process. $E_1$, $\beta_1$ and $E_2$, $\beta_2$ denote the electric field and transport constant of FW pump light and SHW signal light, respectively: (a) $x$-cut LN thin film; (b) $z$-cut LN thin film.

## 3. Numerical Results and Discussion

To achieve highly efficient frequency doubling of 1064 nm in $x$-cut LN waveguide, it is necessary to use the largest nonlinear component $d_{33}$. Therefore, the pump mode and second harmonic mode are TE modes with the same polarization, corresponding to the EL+EL→EL phase-matching scheme. Similarly, in the $z$-cut LN waveguide, both the pump mode

and second harmonic mode are TM modes, corresponding to the EL+EL→EL phase-matching scheme. Assume the top and bottom cladding media are all silica ($n_0 = n_2 = 1.45$). We fix the thickness at 0.982 μm and 0.966 μm for the $x$-cut LN film and $z$-cut LN film, respectively. By solving the eigenvalue of Eq. (1), we can obtain the effective refractive index of different optical modes and find the phase-matching points in the $x$-cut LN thin-film waveguide (all the theoretical formulas used to calculate the $z$-cut LN thin film in this paper can be found in Ref. [17]). The corresponding modal dispersion profiles of FW and SHW with various mode numbers and polarizations are displayed in Fig. 2.

Interestingly, the dispersion curves of different-order waveguide modes in two different tangential LN thin-films have high consistency. The fundamental mode and the second-order SHW mode have a cross point at 1064 nm. Assume the length of the waveguide is 1 cm and the amplitude of FW pump light is $2 \times 10^6$ V/m, a moderate value. The efficiency of SHG in two different types of LN films is calculated and illustrated in Table 1.

We can see that under appropriate waveguide geometry configuration parameters, both the $x$-cut LN thin film and the $z$-cut LN thin film can generate highly efficient frequency doubling of 1064 nm. Moreover, the nonlinear coupling coefficients $\kappa_1$, $\kappa_2$ and the conversion efficiency of two different tangential LN thin-film waveguides are close. This phenomenon can be well explained from the perspective of mode field distribution.

For the $x$-cut LN waveguide, the mode conversion scheme is $\mathrm{TE}_0^{\omega} + \mathrm{TE}_0^{\omega} = \mathrm{TE}_2^{2\omega}$, which contains electric field components $E_x$, $E_{2x}$ and utilizes the largest nonlinear coefficient $d_{33}$. For $z$-cut LN waveguides, the mode conversion scheme is $\mathrm{TM}_0^{\omega} + \mathrm{TM}_0^{\omega} = \mathrm{TM}_2^{2\omega}$, which contains electric field components $E_z$, $E_{2z}$, $E_y$, and $E_{2y}$ and uses nonlinear coefficients $d_{33}$ and $d_{31}$ [17]. As depicted in Figs. 3(a) and 3(b), the normalized mode

**Table 1.** Conversion Efficiency of LN Thin-Film Waveguide.

| | $\lvert\kappa\rvert$ (pm/V) | $\eta$ |
|---|---|---|
| $x$-cut | $\lvert\kappa_1\rvert = 0.199 d_{33} = 5.37$ | 9.27% |
| | $\lvert\kappa_2\rvert = 0.219 d_{33} = 5.91$ | |
| $z$-cut | $\lvert\kappa_1\rvert = 0.248 d_{33} + 0.113 d_{31} = 7.31$ | 13.9% |
| | $\lvert\kappa_2\rvert = 0.243 d_{33} + 0.111 d_{31} = 7.16$ | |

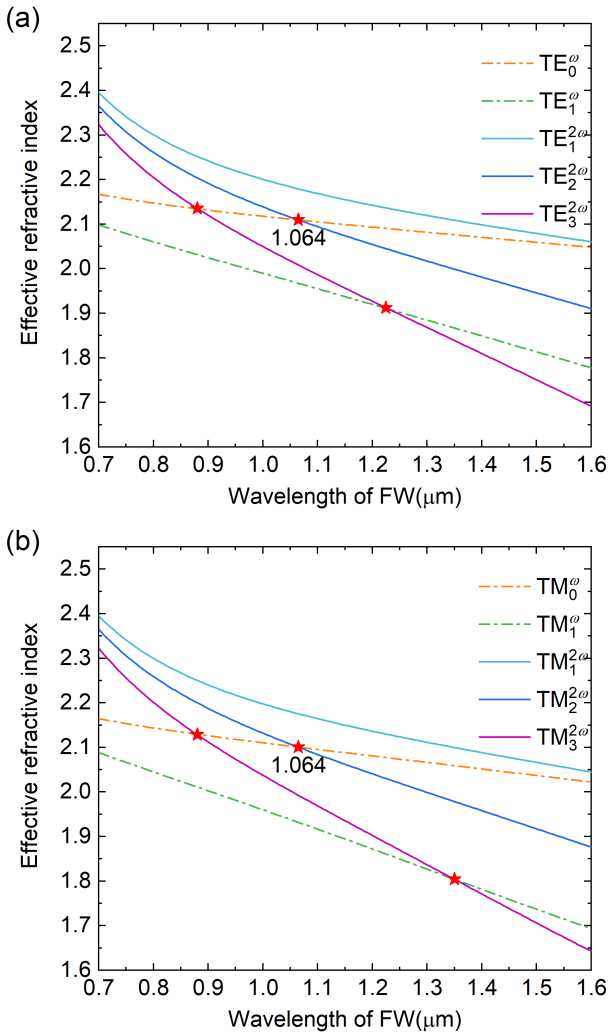


**Fig. 2.** Dispersion curves of EL + EL → EL phase-matching scheme in LN waveguide for various guided modes. The red star point represents the phase-matching point: (a) $x$-cut LN thin film; (b) $z$-cut LN thin film.

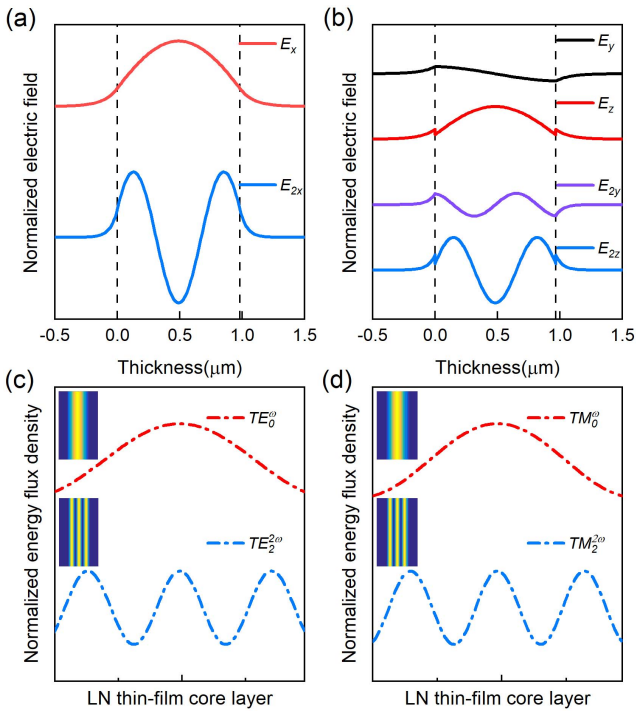


**Fig. 3.** (a) and (b) are normalized electric field distributions in $x$-cut LN thin film and $z$-cut LN thin film, respectively. (c) and (d) are energy flux density diagrams in $x$-cut LN thin film and $z$-cut LN thin film, respectively. The insets are the distributions of light intensity.

field distributions of $E_x$, $E_{2x}$, and $E_z$, $E_{2z}$ are highly consistent, which results in a similar modal overlap integral. Thus, the coefficient before $d_{33}$ is almost the same. However, for the $z$-cut LN thin film, there is one more modal overlap integral term of $E_{2y}$, $E_y$, and $E_z$, which produces a non-negligible contribution from $d_{31}$. As a result, the nonlinear coupling coefficient is bigger than that of the $x$-cut LN thin film and further results in larger conversion efficiency. It can be seen from Figs. 3(c) and 3(d) that the intensity profiles of two different tangential LN thin films also have similar profiles.

It is somewhat astonishing to note that, for two subwavelength LN thin films with almost the same thickness, and whose crystal axes are perpendicular to each other, the conversion efficiencies are comparable and large. We might assume that the MPM and SHG efficiencies of two tangential LN thin films are very robust. Further verifying our conjecture, we change the thickness of the LN thin film and use Eq. (3) to calculate the optimal MPM point and corresponding conversion efficiency in two different types of LN thin-film waveguides.

The result is presented in Fig. 4(a). As the LN thin-film thickness $h$ increases from 0.8 to 2.1 μm, the PM wavelength of the mode conversion scheme $\mathrm{TE}_0^{\omega} + \mathrm{TE}_0^{\omega} = \mathrm{TE}_2^{2\omega}$ in the $x$-cut LN thin film increases from 0.969 to 1.588 μm linearly. Similarly, the PM wavelength of the mode conversion scheme $\mathrm{TM}_0^{\omega} + \mathrm{TM}_0^{\omega} = \mathrm{TM}_2^{2\omega}$ in the $z$-cut LN thin film increases from 0.975

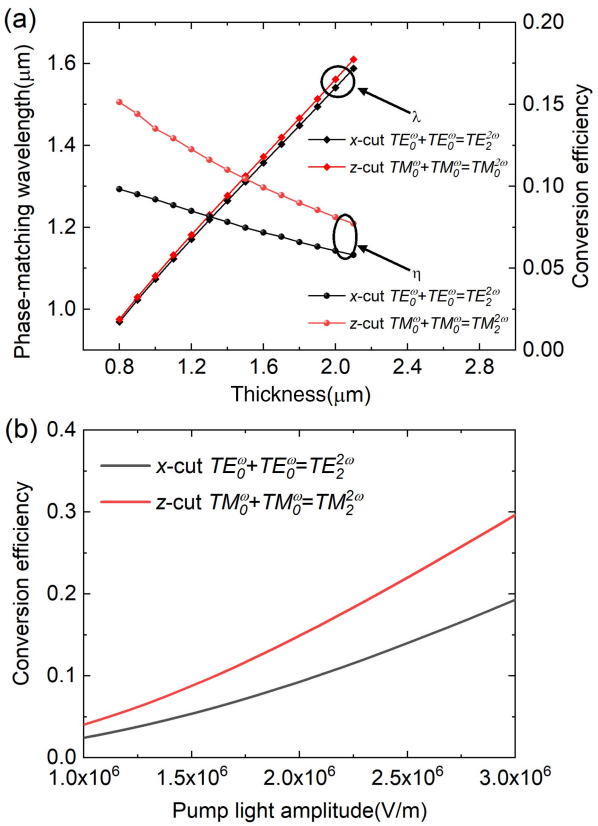


**Fig. 4.** (a) Phase-matching wavelength and efficiency of SHG in dependence on the thickness of LN thin film; (b) dependence of conversion efficiency on FW pump light intensity under large signal conditions.

to 1.610 μm. Both of them cover a wide spectral window, including the 1550 nm telecommunication band. It is worth mentioning that the conversion efficiency decreases almost linearly with the increase of $h$, and this phenomenon can be explained from the standpoint of energy distribution. As the thickness of the LN thin film increases, the field energy density decreases, resulting in lower conversion efficiency. Besides, the conversion efficiency of the two types of LN thin-film waveguides has always stayed in a close range, and the difference between two conversion efficiencies divided by themselves gives a small value, which agrees well with our expectations. Moreover, by enlarging the pump power, it is easy to achieve much higher conversion efficiency. For instance, we select the parameters of the LN thin-film waveguide to be consistent with those used in Fig. 2, and the calculation results are displayed in Fig. 4(b).

## 4. Conclusion

We have used the nonlinear coupled-mode theory to investigate the SHG process in $x$-cut LN thin-film waveguides, made a comparison with the $z$-cut configuration under the MPM scheme, and derived the analytical formulae for calculating the SHG efficiency qualitatively and quantitatively without complicated numerical simulation. We have found appropriate geometric parameters of thin-film waveguides for specific wavelengths as 1064 and 1550 nm and calculated the conversion efficiency of SHG. We are surprised to find that robust MPM exists in subwavelength $x$-cut and $z$-cut LN thin-film waveguides. Under the similar structural parameters of the LN thin-film waveguide, the normalized mode field distribution and modal field overlap integral of $x$-cut and $z$-cut LN thin films are highly consistent, which results in close values for SHG efficiency. By rationally adjusting the geometrical and physical parameters of the LN waveguide, a highly efficient frequency doubling of 1064 nm or other wavelengths can be readily achieved. Such robustness would be very useful for designing, constructing, and applying high-efficiency micro–nano nonlinear optical devices based on the subwavelength LN thin film.

## Acknowledgement

This work was supported by the National Natural Science Foundation of China (No. 11974119), Guangdong Innovative and Entrepreneurial Research Team Program (No. 2016ZT06C594), National Key R&D Program of China (No. 2018YFA0306200), Dongguan Introduction Program of Leading Innovative and Entrepreneurial Talents, and Guangdong Science and Technology Innovation Strategy Special Foundation (No. 2019B090904007).

## References

1. L. Cai, Y. Wang, and H. Hu, "Low-loss waveguides in a single-crystal lithium niobate thin film," Opt. Lett. **40**, 3013 (2015).

2. R. Geiss, S. Saravi, A. Sergeyev, S. Diziain, F. Setzpfandt, F. Schrempel, R. Grange, E.-B. Kley, A. Tünnermann, and T. Pertsch, "Fabrication of nanoscale lithium niobate waveguides for second-harmonic generation," Opt. Lett. **40**, 2715 (2015).
3. A. Rao, J. Chiles, S. Khan, S. Toroghi, M. Malinowski, G. F. Camacho-González, and S. Fathpour, "Second-harmonic generation in single-mode integrated waveguides based on mode-shape modulation," Appl. Phys. Lett. **110**, 111109 (2017).
4. C. Wang, X. Xiong, N. Andrade, V. Venkataraman, X.-F. Ren, G.-C. Guo, and M. Lončar, "Second harmonic generation in nano-structured thin-film lithium niobate waveguides," Opt. Express **25**, 6963 (2017).
5. C. Zhu, Y. Chen, G. Li, L. Ge, B. Zhu, M. Hu, and X. Chen, "Multiple-mode phase matching in a single-crystal lithium niobate waveguide for three-wave mixing," Chin. Opt. Lett. **15**, 091901 (2017).
6. H.-C. Huang, J. I. Dadap, G. Malladi, I. Kymissis, H. Bakhru, and R. M. Osgood, "Helium-ion-induced radiation damage in $LiNbO_3$ thin-film electro-optic modulators," Opt. Express **22**, 19653 (2014).
7. W. Cheng, M. Zhang, B. Stern, M. Lipson, and M. Loncar, "Nanophotonic lithium niobate electro-optic modulators," Opt. Express **26**, 1547 (2017).
8. L. Wang, C. Wang, J. Wang, F. Bo, M. Zhang, Q. Gong, M. Lončar, and Y.-F. Xiao, "High-Q chaotic lithium niobate microdisk cavity," Opt. Lett. **43**, 2917 (2018).
9. Z. Hao, J. Wang, S. Ma, W. Mao, F. Bo, F. Gao, G. Zhang, and J. Xu, "Sum-frequency generation in on-chip lithium niobate microdisk resonators," Photon. Res. **5**, 623 (2017).
10. R. Luo, H. Jiang, H. Liang, Y. Chen, and Q. Lin, "Self-referenced temperature sensing with a lithium niobate microdisk resonator," Opt. Lett. **42**, 1281 (2017).
11. E. S. Hosseini, S. Yegnanarayanan, A. H. Atabaki, M. Soltani, and A. Adibi, "Systematic design and fabrication of high-Q single-mode pulley-coupled planar silicon nitride microdisk resonators at visible wavelengths," Opt. Express **18**, 2127 (2010).
12. S. Diziain, R. Geiss, M. Zilk, F. Schrempel, E.-B. Kley, A. Tünnermann, and T. Pertsch, "Second harmonic generation in free-standing lithium niobate photonic crystal L3 cavity," Appl. Phys. Lett. **103**, 051117 (2013).
13. H. Jiang, H. Liang, R. Luo, X. Chen, Y. Chen, and Q. Lin, "Nonlinear frequency conversion in one dimensional lithium niobate photonic crystal nanocavities," Appl. Phys. Lett. **113**, 021104 (2018).
14. C. Lu, B. Zhu, C. Zhu, L. Ge, Y. Liu, Y. Chen, and X. Chen, "All-optical logic gates and a half-adder based on lithium niobate photonic crystal microcavities," Chin. Opt. Lett. **17**, 072301 (2019).
15. J. A. Armstrong, N. Bloembergen, J. Ducuing, and P. S. Pershan, "Interactions between light waves in a nonlinear dielectric," Phys. Rev. **127**, 1918 (1962).
16. P. A. Franken and J. F. Ward, "Optical harmonics and nonlinear phenomena," Rev. Mod. Phys. **35**, 23 (1963).
17. L.-H. Hong, B.-Q. Chen, C.-Y. Hu, and Z.-Y. Li, "Analytical solution of second-harmonic generation in a lithium-niobate-birefringence thin-film waveguide via modal phase matching," Phys. Rev. A **98**, 023820 (2018).
18. K. Moutzouris, S. Venugopal Rao, M. Ebrahimzadeh, A. De Rossi, M. Calligaro, V. Ortiz, and V. Berger, "Second-harmonic generation through optimized modal phase matching in semiconductor waveguides," Appl. Phys. Lett. **83**, 620 (2003).
19. E. De Luca, R. Sanatinia, M. Mensi, S. Anand, and M. Swillo, "Modal phase matching in nanostructured zinc-blende semiconductors for second-order nonlinear optical interactions," Phys. Rev. B **96**, 075303 (2017).
20. L. Cai, Y. Wang, and H. Hu, "Efficient second harmonic generation in $\chi^{(2)}$ profile reconfigured lithium niobate thin film," Opt. Commun. **387**, 405 (2017).
21. G. J. Edwards and M. Lawrence, "A temperature-dependent dispersion equation for congruently grown lithium niobate," Opt. Quantum Electron. **16**, 373 (1984).
22. M.-L. Ren and Z.-Y. Li, "An effective susceptibility model for exact solution of second harmonic generation in general quasi-phase-matched structures," EPL **94**, 44003 (2011).
23. M.-L. Ren, D.-L. Ma, and Z.-Y. Li, "Experimental demonstration of super quasi-phase matching in nonlinear photonic crystal," Opt. Lett. **36**, 3696 (2011).